Supporting Information

Bioinspired tailoring of nanoarchitectured nickel sulfide@nickel permeated carbon composite as highly durable and redox chemistry enabled battery-type electrode for hybrid supercapacitors

Mohan Reddy Pallavolu,[a] Ramesh Reddy Nallapureddy,[a] Hemachandra Rao Goli,[b] Arghya Narayan Banerjee,[a*] Gutturu Rajasekhara Reddy,[a] and Sang W. Joo[a*]

[a]*School of Mechanical Engineering, Yeungnam University, Gyeongsan 38541, Republic of Korea*
[b]*Department of Physics, Banasthali University, Banasthali, Rashathan-304022, India*

Corresponding authors:

Arghya Narayan Banerjee (arghya@ynu.ac.kr; banerjee_arghya@hotmail.com);

Sang W. Joo (swjoo@yu.ac.kr)

Table S1: Crystallographic data of NiS

Parameters	**NiS**
Crystal system	Rhombohedral
Space group	*R3m*
Space group number	160
a **(Å)**	9.62
b **(Å)**	9.62
c **(Å)**	3.15
α **(deg.)**	90.0
β **(deg.)**	90.0
γ **(deg.)**	120
Reference	JCPDS ICDD 00-012-0041

Table S2. Comparative electrochemical properties of wheat snack-derived NiS-Ni@C composite with recently reported redox-active materials.

Materials	**Electrolyte**	**Current density ($A\ g^{-1}$)**	**Specific capacity**	**Ref.**
FeS_x/C/CNT	3 M KOH	1	370.5 C g^{-1}	[1]
NiS_2/CNTs	2 M KOH	1	354 C g^{-1}	[2]
CFC/NiS_2/PC	2 M KOH	1	424.5 C g^{-1}	[3]
Ni_3S_2@NC	2 M KOH	2	205.4 C g^{-1}	[4]
$NiCo_2S_4$/GA	3 M KOH	1	380.3 C g^{-1}	[5]
FeS_2/graphene aerogel	6 M KOH	0.5	188.2 C g^{-1}	[6]
Ni_2P/Ni/C	2 M KOH	1	257.2 C g^{-1}	[7]
CoS_2/CNFs	6 M KOH	1	244 C g^{-1}	[8]
3DCoS/graphene composite hydrogel	6 M KOH	1	253.8 C g^{-1}	[9]
CuS/GO	3 M KOH	0.5	150 C g^{-1}	[10]
Ni@NC	3 M KOH	0.5	224 C g^{-1}	[11]
NiS-Ni@PC	2 M KOH	1	430 C g^{-1}	This work

Table S3. Comparable energy and power densities of previously reported device with our hybrid nanocomposite-based HSC.

Device configuration	Electrolyte	Energy density (Wh/kg)	Power density (W/kg)	Ref.
NiS-HS//AC	2 M KOH	24.8	150	[12]
Ni_3S_4//AC	2 M KOH	18.625	150	[13]
NiS HNPs//AC	2 M KOH	11.6	187.5	[14]
NiS@C//C	2 M KOH	21.6	400	[15]
PHCSs/NiS//AC	6 M KOH	24.4	767	[16]
Ni_3S_2/MWCNT-NC//AC	2 M KOH	19.8	798	[17]
$NiCo_2S_4$/CFP//AC	2 M KOH	17.3	180	[18]
NiCoS@N-pCNFs//AC@N-pCNFs	3 M KOH	21.7	134.9	[19]
MoS_2/Ni_3S_2//rGO	6 M KOH	21.8	400	[20]
NiS-Ni@C//AC	2 M KOH	28.1	380	This work

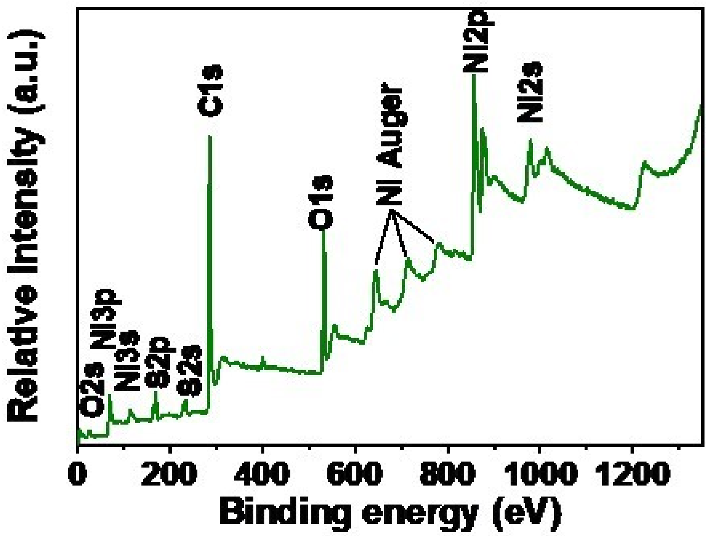

Figure S1. XPS survey spectra of $NiS_{1.2}$-Ni@PC

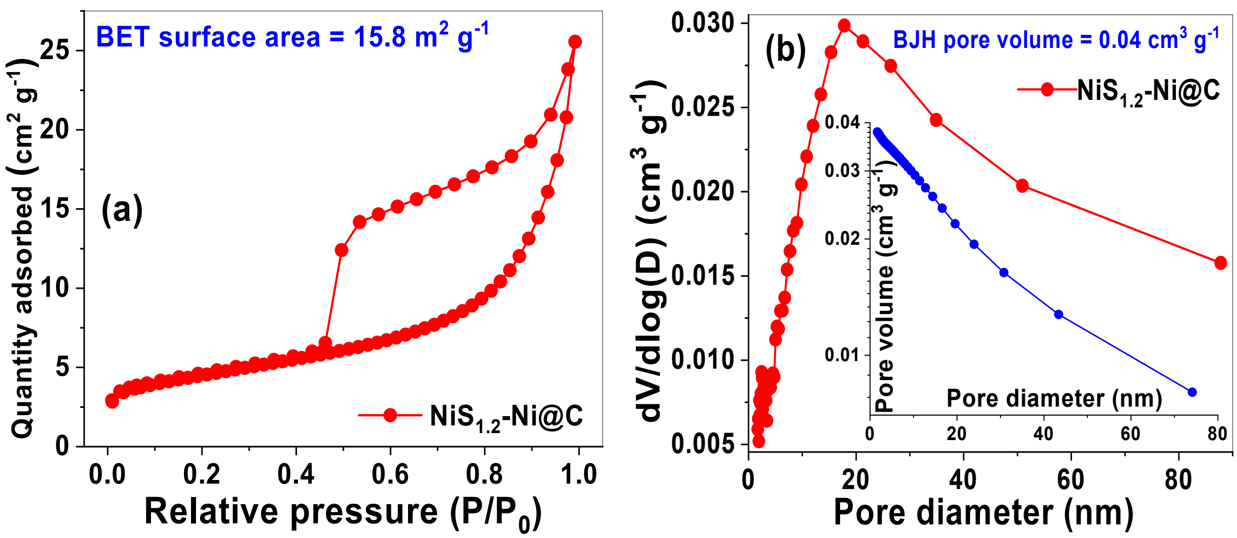

Figure S2. (a) N_2 adsorption-desorption isotherm and (b) BJH pore size distribution of $NiS_{1.2}$-Ni@C (Inset: Pore volume vs. pore diameter).

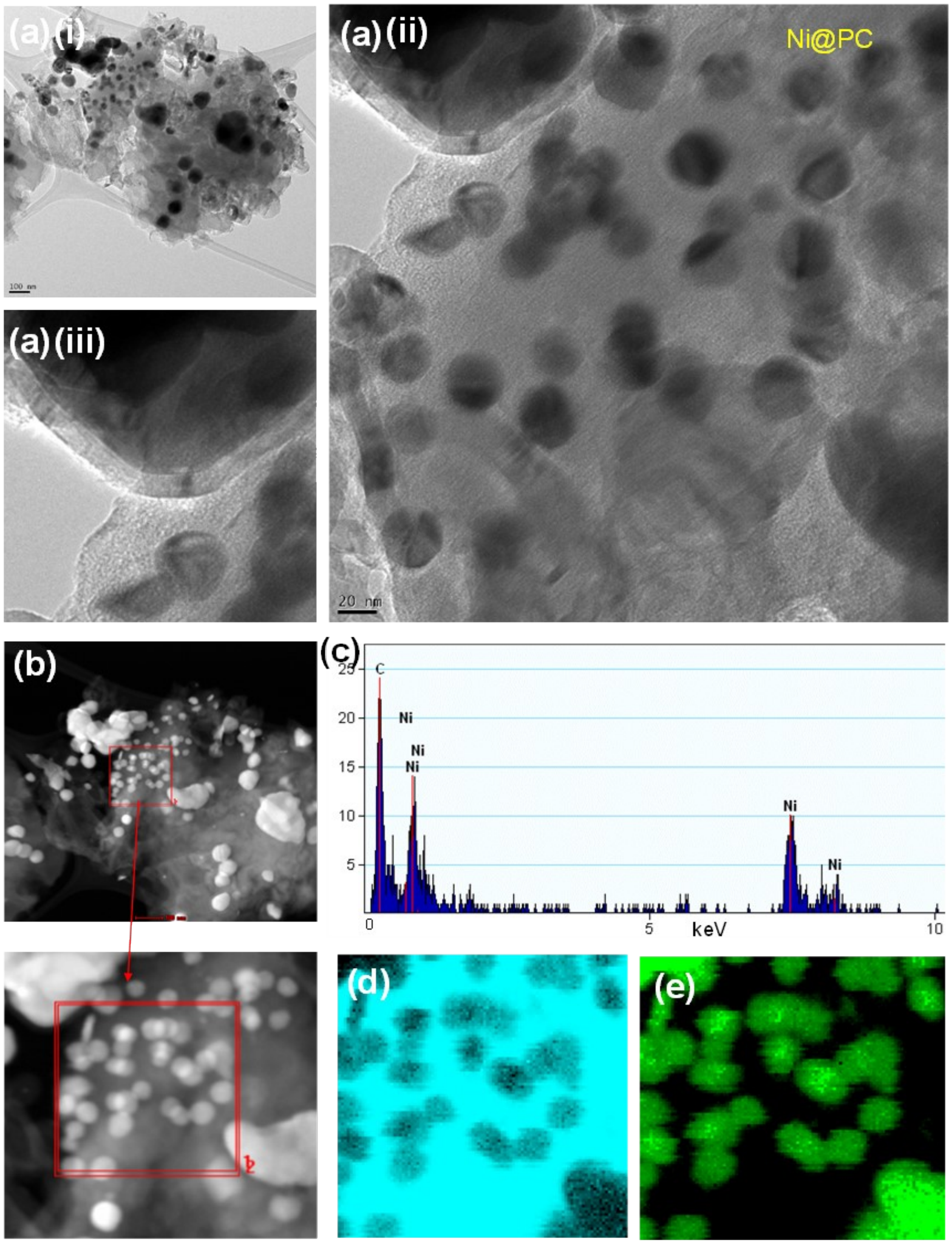

Figure S3. (a)(i-iii) Low- and high-magnification TEM images of Ni@C and (b-e) EDX spectra and elemental mapping images of Ni@C showing the respective elements of C and Ni.

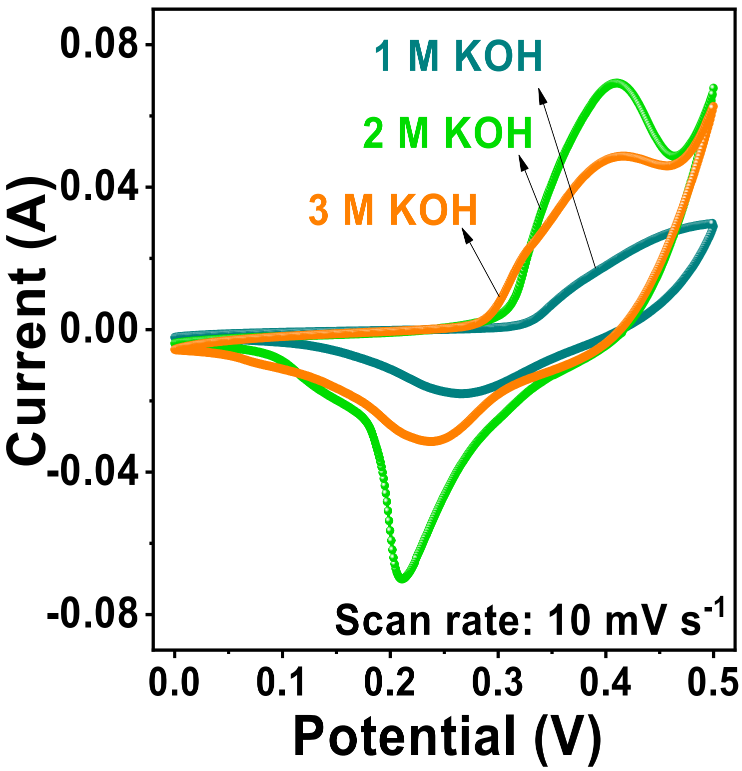

Fig. S4. CV plots of $NiS_{1.2}$-Ni@C electrode at different electrolyte concentrations.

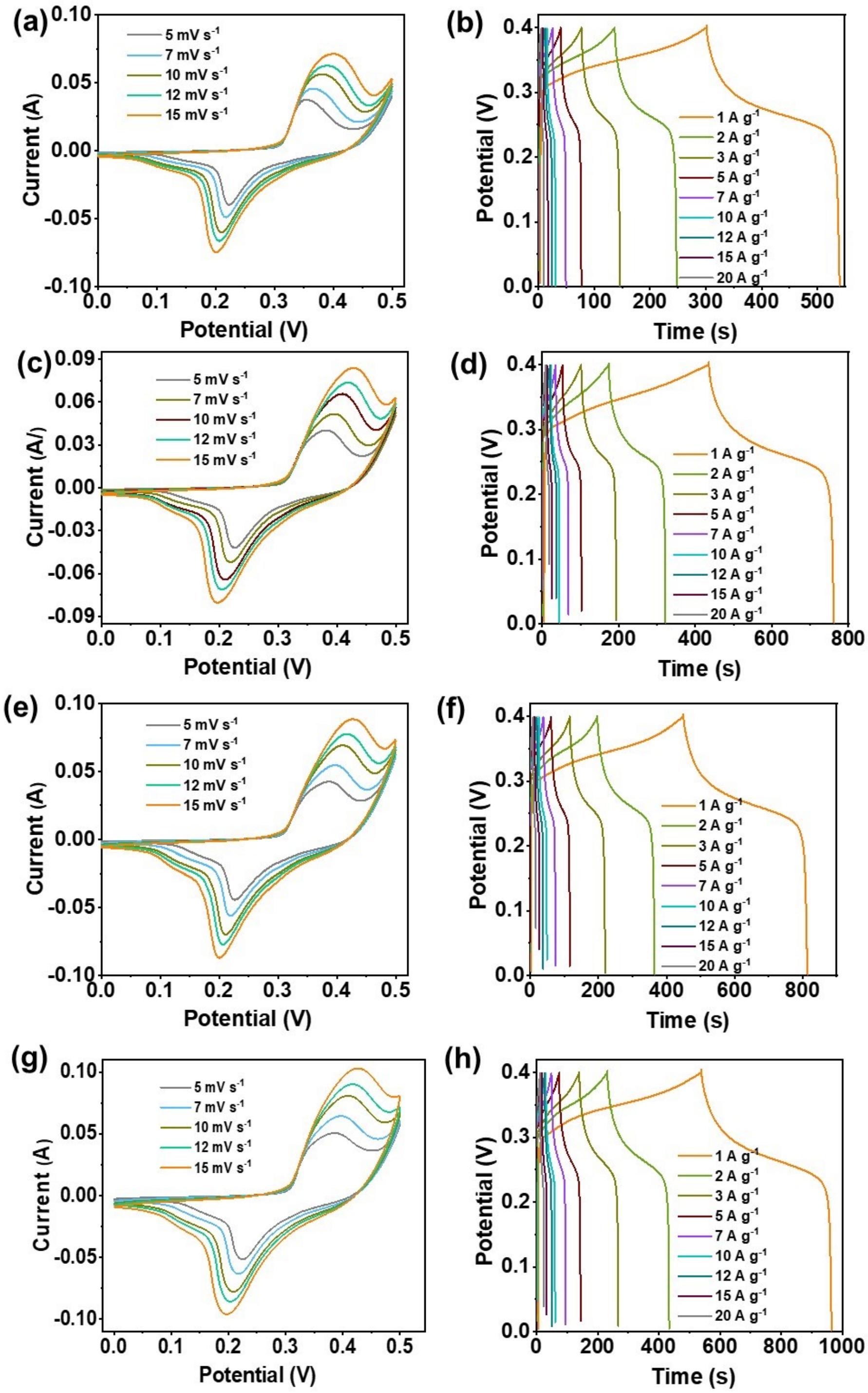

Figure S5. CV and GCD curves of (a-b) Ni@PC, (c-d) $NiS_{0.4}$-Ni@PC, (e-f) $NiS_{0.8}$-Ni@PC, and (b-c) $NiS_{1.2}$-Ni@PC samples measured at different scan rates (5-15 mV s^{-1}) and current densities (1-20 A g^{-1}), respectively.

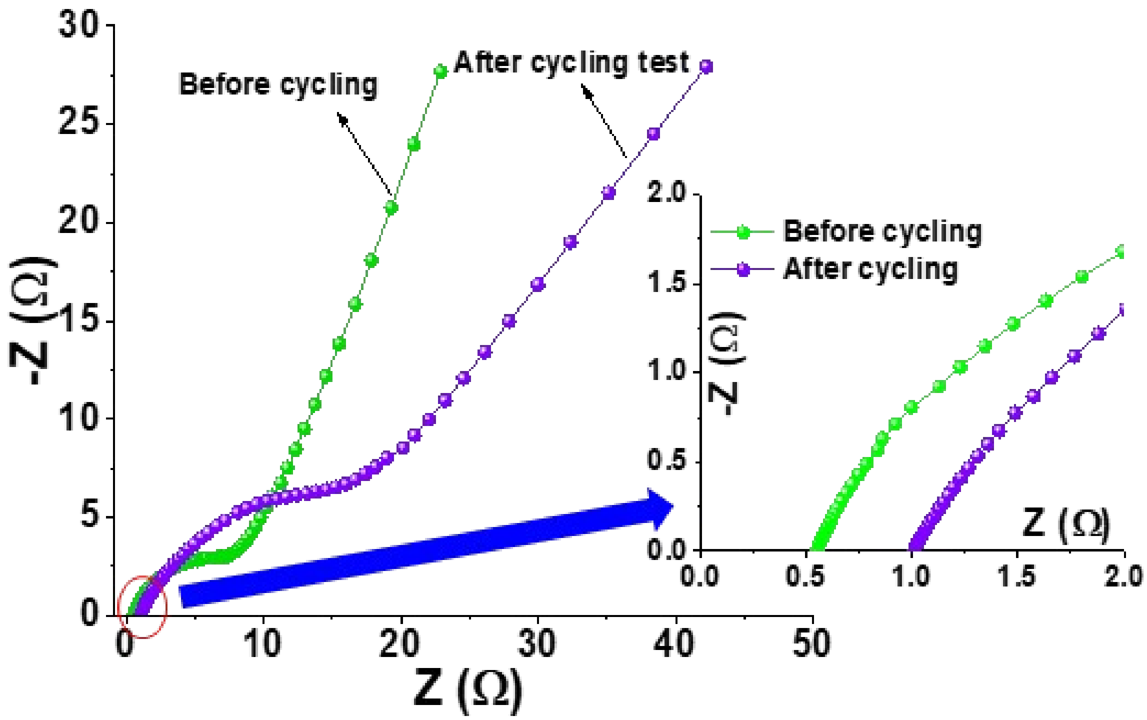

Fig. S6. Nyquist plots of $NiS_{1.2}$-Ni@C electrode before and after 5000 cycles. An increase in the R_s value is observed after 5000 cycles. Also, the diameter of the semicircular portion is increased after cycling, indicating an increase in the R_{ct} value. Also, the low-frequency linear part is slanted from a ~75^O to ~60^O angle (against *x*-axis), revealing an increase in the diffusion resistance after cycling.

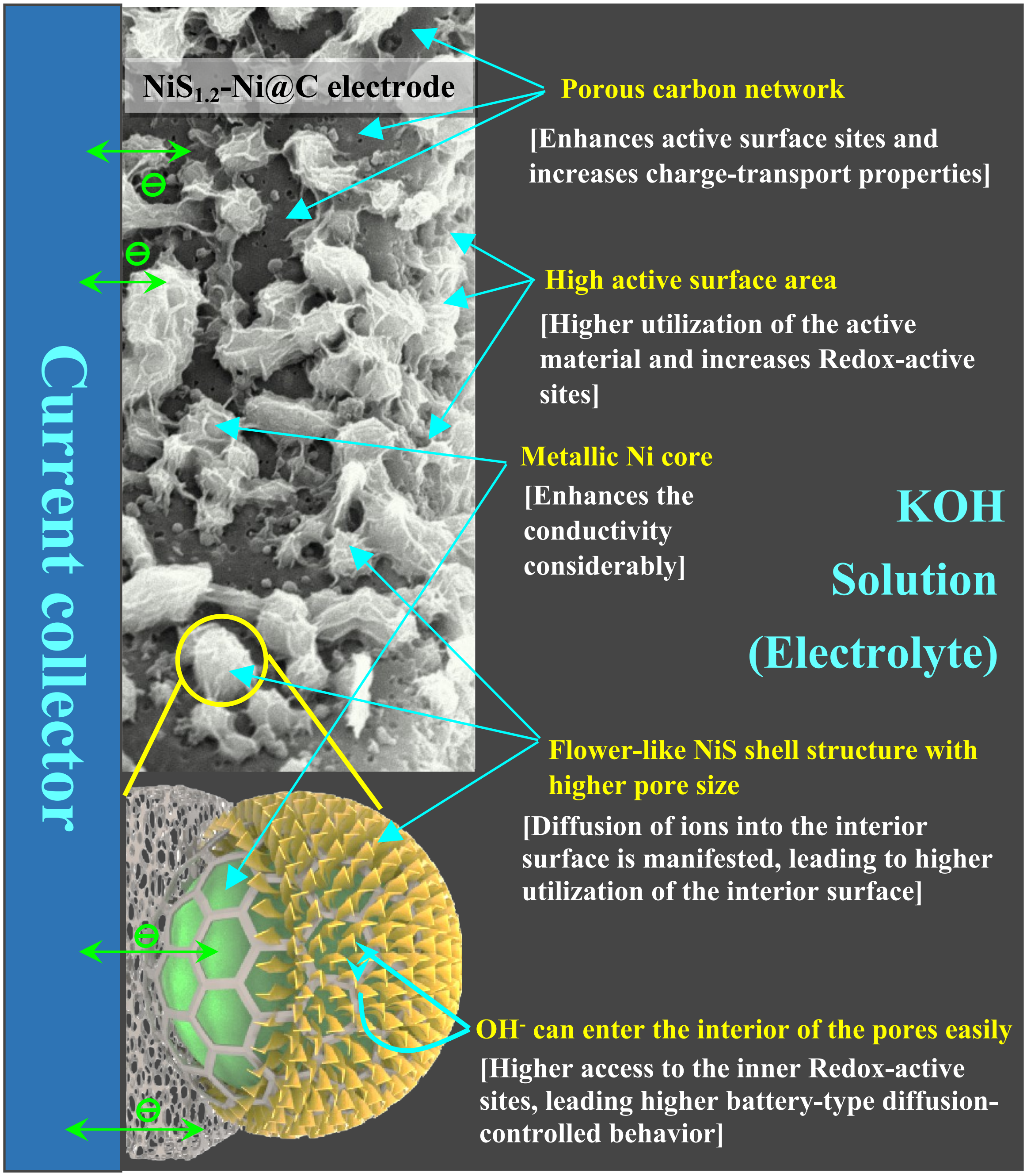
NiS1.2-Ni@C electrode
Current collector
Porous carbon network
[Enhances active surface sites and increases charge-transport properties]
High active surface area
[Higher utilization of the active material and increases Redox-active sites]
Metallic Ni core
[Enhances the conductivity considerably]
KOH Solution (Electrolyte)
Flower-like NiS shell structure with higher pore size
[Diffusion of ions into the interior surface is manifested, leading to higher utilization of the interior surface]
OH- can enter the interior of the pores easily
[Higher access to the inner Redox-active sites, leading higher battery-type diffusion-controlled behavior]

Fig. S7. Schematic illustration of the enhanced electrochemical performance of the NiS-Ni@C electrodes.

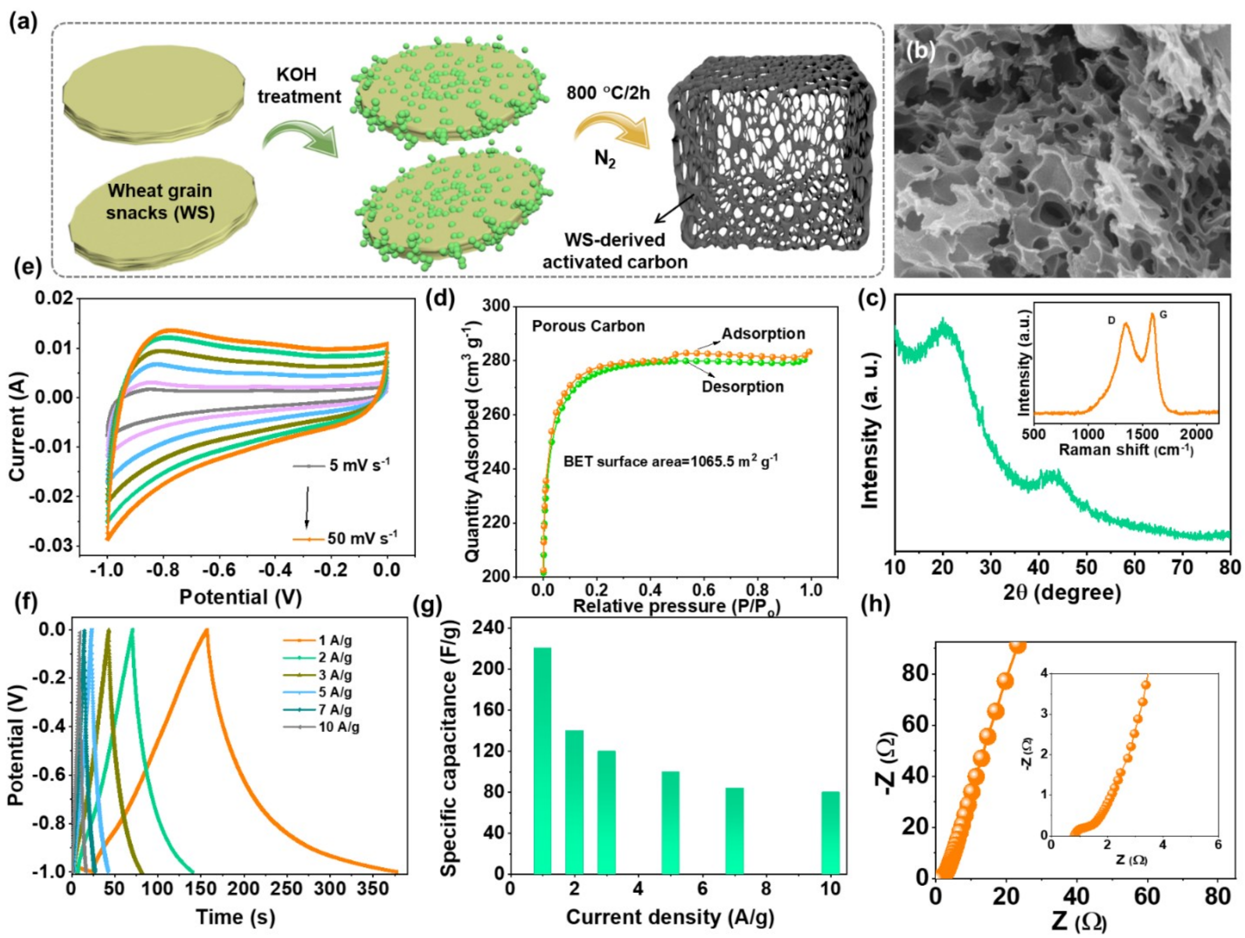

Figure S8. a) Schematic illustration showing the synthesis process of wheat snack derived activated carbon, b) SEM image of porous carbon, c) XRD with inset Raman spectra of PC, d) Nitrogen adsorption/desorption isotherms, e) CV profiles at different scan rates of 5 – 50 mV s^{-1}, f) GCD profiles at different current densities from 1 – 7 A g^{-1}, g) Specific capacitance values calculated from GCD data, and h) Nyquist plot of PC (Inset: Same plot at high frequency region).

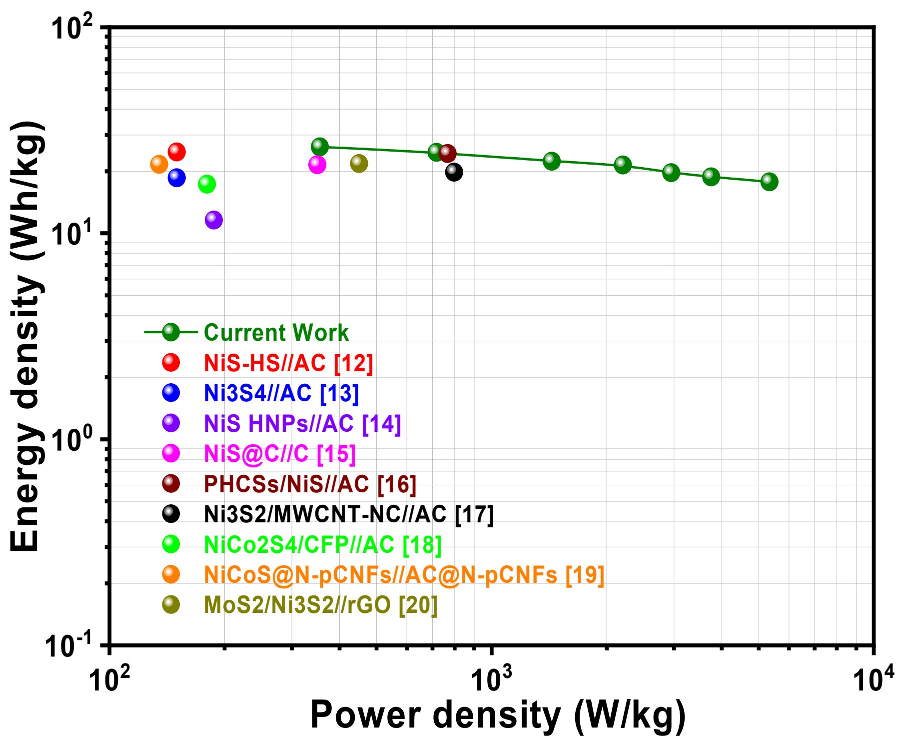

Fig. S9. Comparison of the energy-power performance of our device against various other hybrid composite-based device reported in the literature.

References

[1] Y. Zhang, M. Xu, Y. Wang, S. Lin, L. Ji, X. Li, Y. Zhang, J. Zhao, *Journal of Alloys and Compounds* **2020**, *834*, 154916.

[2] X. Lei, M. Li, M. Lu, X. Guan, *Materials* **2019**, *12*, 3509.

[3] J.-B. Fang, C. Liu, Y.-Q. Cao, A.-D. Li, *Journal of Materials Research* **2020**, *35*, 738.

[4] M. Kumar, D. I. Jeong, N. Sarwar, D. H. Yoon, *Ceramics International* **2021**, *47*, 16852.

[5] B. Li, Z. Tian, H. Li, Z. Yang, Y. Wang, X. Wang, *Electrochimica Acta* **2019**, *314*, 32.

[6] L. Pei, Y. Yang, H. Chu, J. Shen, M. Ye, *Ceramics International* **2016**, *42*, 5053.

[7] Y. Xu, S. Xiong, S. Weng, J. Wang, J. Wang, H. Lin, Y. Jiao, J. Chen, *New J. Chem.* **2020**, *44*, 6810.

[8] Z. Wang, C. Liu, G. Shi, G. Wang, Q. Zhang, H. Zhang, Y. Su, J. Yu, X. Li, F. Luo, Y. Hu, K. Yi, *Ionics* **2020**, *26*, 5737.

[9] X. Meng, J. Deng, J. Zhu, H. Bi, E. Kan, X. Wang, *Scientific Reports* **2016**, *6*, 21717.

[10] R. Singhal, D. Thorne, P. K. LeMaire, X. Martinez, C. Zhao, R. K. Gupta, D. Uhl, E. Scanley, C. C. Broadbridge, R. K. Sharma, *AIP Advances* **2020**, *10*, 035307.

[11] K. Wang, Z. Wang, J. Liu, C. Li, F. Mao, H. Wu, Q. Zhang, *ACS Appl. Mater. Interfaces* **2020**, *12*, 47482.

[12] T. Liu, C. Jiang, B. Cheng, W. You, J. Yu, *J. Mater. Chem. A* **2017**, *5*, 21257.

[13] H. Wang, M. Liang, D. Duan, W. Shi, Y. Song, Z. Sun, *Chemical Engineering Journal* **2018**, *350*, 523.

[14] Z. Li, X. Yu, A. Gu, H. Tang, L. Wang, Z. Lou, *Nanotechnology* **2017**, *28*, 065406.

[15] J. Wu, F. Wei, Y. Sui, J. Qi, X. Zhang, *International Journal of Hydrogen Energy* **2020**, *45*, 19237.

[16] D. Wu, H. Yu, C. Hou, W. Du, X. Song, T. Shi, X. Sun, B. Wang, *J Mater Sci* **2020**, *55*, 14431.

[17] C.-S. Dai, P.-Y. Chien, J.-Y. Lin, S.-W. Chou, W.-K. Wu, P.-H. Li, K.-Y. Wu, T.-W. Lin, *ACS Appl. Mater. Interfaces* **2013**, *5*, 12168.

[18] X. Xiong, G. Waller, D. Ding, D. Chen, B. Rainwater, B. Zhao, Z. Wang, M. Liu, *Nano Energy* **2015**, *16*, 71.

[19] Y. Liu, Q. Lu, Z. Huang, S. Sun, B. Yu, U. Evariste, G. Jiang, J. Yao, *Journal of Alloys and Compounds* **2018**, *762*, 301.

[20] L. Huang, H. Hou, B. Liu, K. Zeinu, X. Zhu, X. Yuan, X. He, L. Wu, J. Hu, J. Yang, *Applied Surface Science* **2017**, *425*, 879.